CARBON NANOTUBE COMPOSITE SCAFFOLDS FOR DIFFERENTIATION OF HUMAN NEURAL STEM CELLS

By

GREGORY HEDEN

A thesis submitted to the

Graduate School – New Brunswick

Rutgers, The State University of New Jersey

in partial fulfillment of the requirements

for the degree of

Masters of Science

Graduate Program in Chemical Engineering

written under the direction of

Professor Alexander V. Neimark

And approved by

_____

_____

_____

New Brunswick, New Jersey

May 2013

ABSTRACT OF THE THESIS

Carbon Nanotube Composite Scaffolds for Differentiation of Human Neural Stem Cells

By GREGORY HEDEN

Thesis Director:

Professor Alexander V. Neimark

Carbon nanotubes have been utilized in a variety of fields due to their unique and extraordinary properties. Here, a process to incorporate single-walled carbon nanotubes (SWNTs) into electrospun polymer mats is investigated in order to create novel composite scaffolds to enhance the differentiation of human neural stem cells (hNSCs) into fully developed neurons. An electrowetting method is first explored using a potential difference as a driving force. Although successful wetting was achieved, a vacuum impregnation method was used to further improve the uniformity of the SWNT distribution in the scaffold. This process produced homogenously wetted scaffolds that are electrically conductive, mechanically robust, and highly biocompatible with hNSC cultures *in vitro*. These scaffolds showed an increased expression of two major neuronal markers, Neurofilament M (NFM) and microtubule-associated protein-2 (MAP2) compared to plain electrospun polymer scaffolds. During differentiation tests, an additional electrical stimulation was applied and showed even further enhancement. This is the first demonstration of electrical stimulation enhancing neuronal differentiation of human neural stem cells on CNT-based composite scaffolds.

Acknowledgements

I would like to thank my advisor Professor Alexander V. Neimark for his helpful guidance and support throughout my time as a student. I am extremely grateful he accepted me into his research group and granted me the freedom to explore and accomplish my goals in the lab and at Rutgers. I would especially like to thank Dr. John Landers, a PhD student of Dr. Neimark's at the time, who allowed me to participate in his research as an undergraduate. His experience and encouragement motivated me to become a better scientist and student. I was honored to be able to continue his research after he completed his PhD. In addition to my advisor I would like to thank and acknowledge members of my committee: Dr. Prabas Moghe for his invaluable critiques and advice and Dr. Tewodros (Teddy) Asefa for his expertise and helping with my defense. I would also like to acknowledge the members of Professor Neimark's group for sharing their knowledge, assistance, critiques and time during my stay in the group: John Landers, Chris Rasmussen, Ming-Tsung Lee, Richard Cimino, Aleksey Vishnyakov, and Parag Shah. I would also like to thank a number of graduate students who, be it through friendship, helpful discourse, or imparting experience have greatly impacted my experience here at Rutgers: Jeffrey Turner, Aaron Carlson, Neal Bennett, and Benjamin Groth. I would like to thank Dr. Gerardo Callegari for his enthusiasm and support. I would also like to thank Dr. Benjamin Glasser for the use of his lab and Valentin Starovyotov for his help with the scanning electron microscope. Finally, I would like to thank my family who has been very supportive and available during my progression as a student.

Table of Contents

LIST OF FIGURES

Chapter I – Introduction

Nano carbon materials have continued to be of increasing interest in the past three decades since the discovery of fullerenes in 1985 [1]. The discovery of new allotropes of carbon soon followed including carbon nanotubes (CNTs) in 1991 [2] and graphene in 2004 [3]. CNTs have gained much popularity do to their extraordinary mechanical and electric properties. They have been reported to have 10-100 times the strength of the strongest steal at a fraction of the weight and an elastic modulus comparable to that of diamonds (>1 TPa). The high aspect ratio (1000:1) and large surface area (~1300 m^2/g) puts it on par with many activated carbons. The superior conductivity of CNTs also allows a current carrying capacity estimated to be 1000 times greater than that of copper wires [4]. In addition, it has been shown that CNTs are biocompatible [5-7]. As a result, CNTs have since been employed into a variety of different research fields [8].

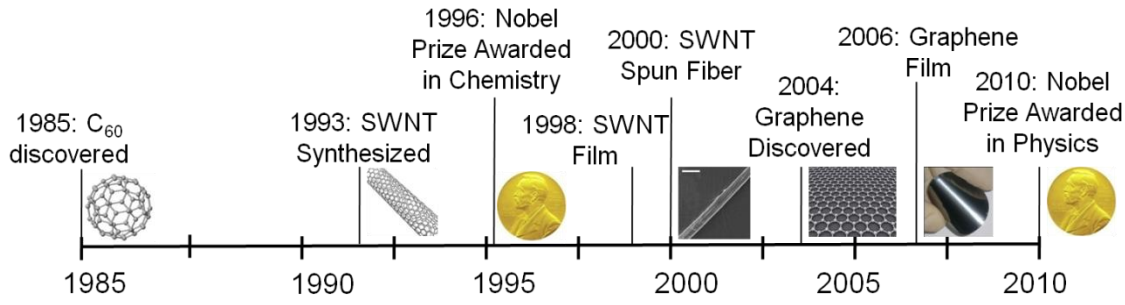

Figure 1-1: Timeline of nanocarbon materials.

In this work, the advantages of single walled carbon nanotubes (SWNT) are applied to enhance the differentiation of human neural stem cells. The first objective behind this was to incorporate a dispersion of SWNT into a fibrous polymer scaffold that mimics the extracellular matrix to promote differentiation into fully developed neurons.

The next objective was to show how this scaffold improved the differentation results by comparing the process with other substrates. Collaboration between the Rutgers Chemical Engineering department and Biochemical Engineering department focused on the materials aspect and cell studies, respectively. When I started working on this project under the direction of Dr. Alexander V. Neimark and his PhD student John Landers, an electrowetting process was explored to force the aqueous SWNT dispersion into the hydrophobic polymer scaffold. I improved this process by redesigning the electrode to have more evenly aligned contact points and a more firm apparatus. This greatly improved the wetting results of the scaffolding by giving a more homogenous product. The limitations of electrowetting however still did not provide the complete uniformity desired for the application of stem cell differentiation. To further improve this wetting process, I suggested that we reexplore a vacuum forced impregnation method using filters with smaller pore size. After being provided 0.2μm filters from John Landers, I was successfully able to develop a system to produce homogenous, completely wetted scaffold products with an easy to replicate method. After being instructed by John Landers on how to operate the scanning electron microscope and Raman spectrometer, I was able to confirm the presence of SWNT in the scaffolds. These scaffold products were delivered to Dr. Prabhas Moghe's group, where his students to Jeffrey Turner and Aaron Carlson performed the biological side of the experiments. An applied electrical stimulation to the scaffold was also discussed by the collaboration to further enhance the differentiation as evident from the literature. To do this, I built a circuit board capable of stimulating up to eight samples simultaneously. I also etched ITO glass slides to act as electrodes when bridged with the conductive scaffold samples. The results obtained from

the collaboration showed that these scaffolds had an enhanced effect on human neural stem cell differentiation and lead to a paper submission. In Chapter 2 of this thesis, fabrication and characterization techniques of the carbon and polymer substrate will be discussed. Chapter 3 will then explore the biological application of these scaffolds and its effect on the differentiation of human neural stem cells. Finally Chapter 4 will conclude and express any future work that may be done in order to further improve the findings in this thesis.

Chapter II – Fabrication of Nanocarbon Composites

II.1 Carbon Nanotube Dispersion

SWNTs were first synthesized by Iijma in 1993 [9]. They can be described as a rolled up sheet of one atom thick graphene comprised of hexagonally bonded sp^2 carbon atoms. The pi-pi orbital interactions on the surface of carbon nanotubes are responsible for the accumulation of van der Waals forces that result in the high mechanical strength, high aspect ratio, inert structural properties and superior conductivity. Aggregation of carbon nanotubes into bundles is a consequence of these forces developing a deep energetic well. In order to take full advantage of these properties, SWNT must be separated.

Ultrasonication with a surfactant or polymer is a popular method for separating SWNT bundles in a dispersion [10]. The surfactant acts as a stabilizing agent when incorporated between the individual tubes through micelle formation or random adsorption, preventing reagglomeration of the CNTs (**Figure 2-1**). In this work, the protein bovine serum albumin (BSA) has been chosen as a stabilizing agent. Proteins disperse CNT by physically wrapping around them, leading to a strong electrostatic and nonspecific adsorption [11, 12]. BSA is also commercially available and abundantly cheap. Most importantly, the structure of BSA is very similar its human counterpart, which is one of the most prolific proteins in the body. This makes materials incorporating BSA less likely to be recognized by the host's immune system [13].

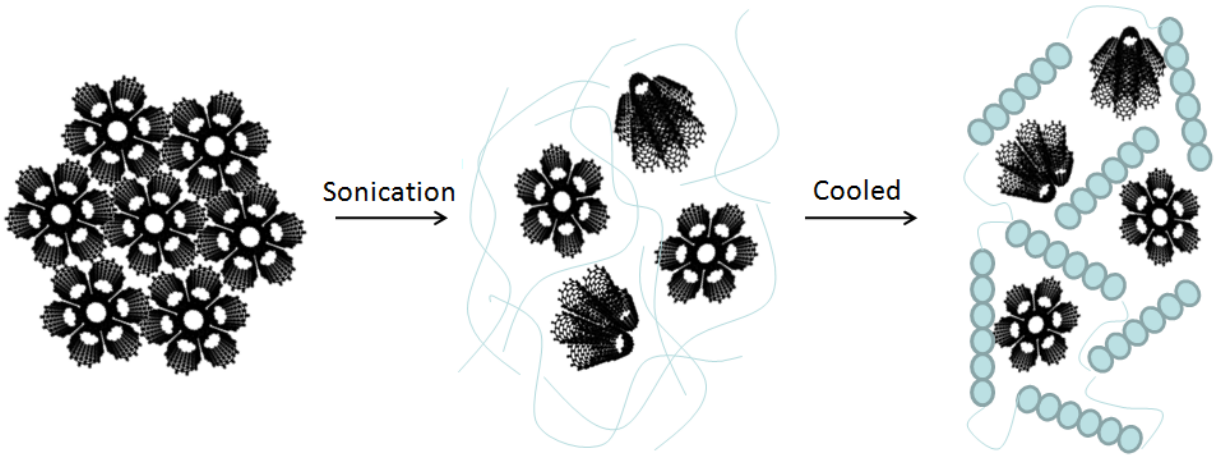

Figure 2-1: Schematic of dispersion mechanism for aggregates of carbon nanotube bundles. Upon sonication, there is enough shear to be imparted to the aggregated bundles to separate them.

The aqueous carbon nanotube dispersion in this work was composed of a 1:1:1 ratio by mass of SWNT (Unidym), BSA (Sigma-Aldrich), and ascorbic acid (Sigma-Aldrich). The dispersion was mixed with a horn tip sonicator (Mixsonix S400) for 10 minutes at a pulsed rate of one second on and one second off at 40 amperes. Dispersions containing 0.4 (wt% by vol) of SWNT was used for the differentiation tests, but other concentrations were also explored for scaffold characterization.

II.2 Polymer Scaffolds

There exists a variety of techniques for the fabrication of scaffolds for neural stem cell differentiation. One popular route for developing polymeric scaffolds is through the process of electrospinning. In this process a polymer solution is dispensed by a syringe towards a charged plate or charged rotating mandrel separated by some distance. When a difference in voltage is applied, a charge separation occurs within the polymer solution causing it to extrude out of the syringe in a fiber form. Once this fiber lands on the charged plate, the polymer solvent quickly evaporates and the fiber solidifies. After sometime this process creates a polymeric and porous scaffold. The elecrospinning

process offers a high degree of control of diameter, density, elastic modulus, and fiber alignment, allowing for the ability to customize the scaffold to directly mimic the three-dimensional topography of the extracellular matrix (ECM) [14].

Here, scaffolds were made with the copolymer poly(lactic-co-glycolide) (PLGA). 15 (wt% by vol) PLGA (Sigma-Aldrich, 85:15 PLA:PGA) was dissolved in 1,1,1,3,3,3-Hexafluoro-2-propanol (Sigma-Aldrich, HFIP) with gentle agitation. This solution was electrospun with a potential difference of +18kV and a 23 gauge needle at a distance of 18cm onto a grounded flat plate collector. The fibrous scaffold products were placed in a vacuum to dry overnight.

Attempts have been made to implement conductive materials, such as CNT, into this process. However the presence of conductive materials within the polymeric solution can cause a shorting to occur and prevent the formation of the fiber extruding from the syringe. This is indeed the case as a review of the literature reveals only a few instances [15-19] where the electrospinning with trace amounts of CNT did not proceed without the use of multi walled carbon nanotubes (MWNT) or functionalized single walled carbon nanotubes (f-SWNT). This is a critical concern because in both cases the conductivity is hindered compared to their non-functionalized SWNT counterpart. The decrease in conductivity from the use of MWNT can be attributed to their decrease in curvature. The f-SWNT conductivity is reduced by a covalent disruption of the highly overlapped pi-pi orbital surface. Therefore the purpose of this work is to demonstrate a post fabrication technique that enables the integration of non functionalized SWNT into polymeric scaffolds. Two methods were explored to incorporate the dispersion into the hydrophobic scaffolds: electrowetting and vacuum impregnation.

II.3 Electrowetting of Scaffolds

The electrowetting process has long been utilized to impregnate a porous substrate with a nonwetting fluid. An electrode is placed into a droplet of the aqueous SWNT dispersion on the hydrophobic polymer scaffold. A thin layer of insulation rests between the scaffold and the metallic base in which another electrode is fastened. When a voltage is applied at the droplet, the attraction to the counter electrode decreases the contact angle between the droplet and scaffold. The change in interfacial properties forces the droplet into the scaffold. Continuation of the applied voltage results in the impregnation of the scaffold, evident by the fact that the dispersion has penetrated to the opposite side.

The application of the voltage to the conductive dispersion transforms the scaffold into a parallel plate capacitor. The fundamental Lippmann equation can be used to approximate the parallel capacitor for the droplet-dielectric interface [20, 21]:

(Eq. 2.1)

where γ_{SL} is the interfacial tension between the scaffold and the liquid, V is the applied voltage, and σ is the surface charge density. This surface charge density is composed of the capacitance, C, with cross sectional area A. The equilibrium contact angle, or Young's angle, is calculated from a force balance at the contact line. The resulting equation is Young's equation,

(Eq. 2.2)

where θ is Young's angle and γ_{LV}, γ_{SV}, and γ_{SL} are surface tensions at the liquid-vapor, solid-vapor, and solid-liquid interfaces, respectively. Combining Young's equation and the fundamental Lippmann equation gives

(Eq. 2.3)

The above equation can be integrated to the Lippmann condition for electrowetting:

(Eq. 2.4)

where θ_0 is the contact angle absent an applied voltage. Since $C = \varepsilon_0\varepsilon_1 A/d$, where ε_1 and ε_0 is the dielectric constant with and without an applied electric field, respectively and d is the scaffold thickness, the voltage required to affect the contact angle is thus:

(Eq. 2.5)

II.4 Electrowetting Apparatus

The electrowetting setup consists of a power source, a custom designed electrode, and an aluminum base. A layer of plastic insulation rests between the top of the base and the polymer scaffolding. Wires from the power source are connected to the metal base, the electrode, and a ground source to prevent shorting. Droplets of the dispersion are dispensed evenly onto the scaffold. The multipinned electrode is carefully lined up and lowered into the droplets. When voltage is applied, it can be immediately seen that the dispersion begins to wet the surface evident by the change in contact area (**Figure 2-2**). The voltage may be gradually increased until a dielectric breakdown occurs.

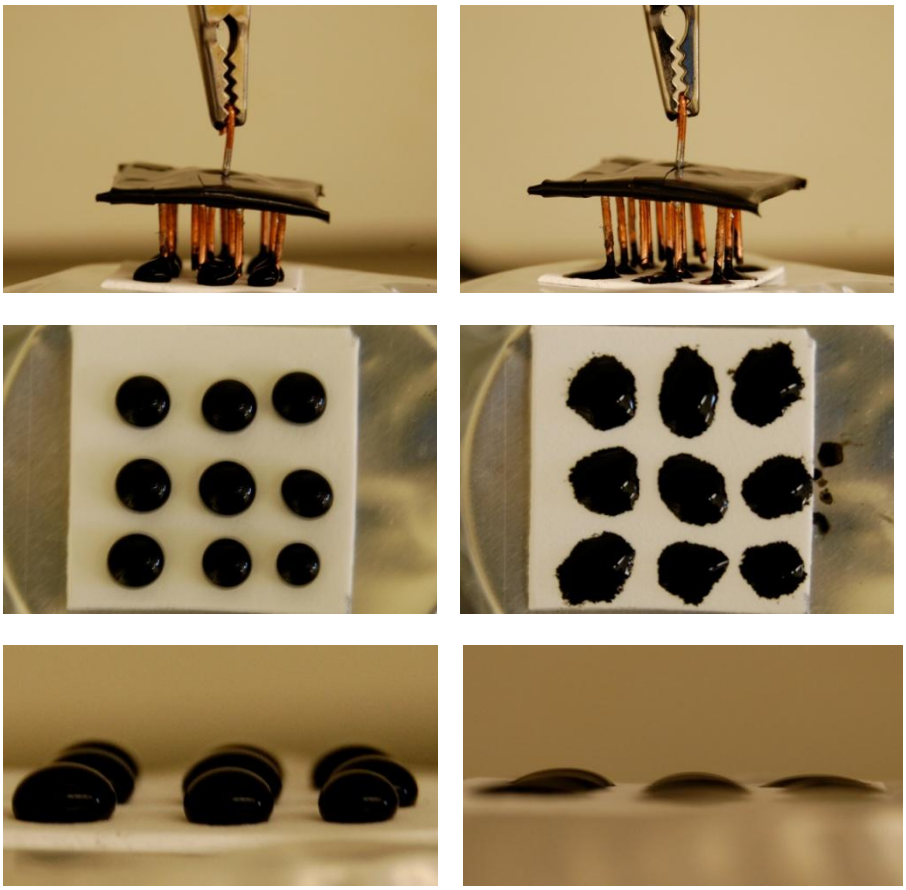

Figure 2-2: Earlier prototype of multi pin electrode used to electrowet and corresponding top and side view images of droplets prior to electrowetting (left) and after electrowetting (right). Substrate consists of porous Teflon as a test model for the scaffolds.

Throughout the timeline of the electrowetting experiments, the electrode and setup underwent modification to further adjust and enhance the wetting ability (**Figure 2-3**). A new electrode was designed with more contact points closer together. Also, the addition of many small drops onto the scaffold to form a thin layer of dispersion produced a more uniform product. Although these alterations drastically improved the wetting of the scaffold (**Figure 2-4**), the still inhomogeneous nature of the dispersion in the scaffold made electrowetting an ineffective method for the desired application.

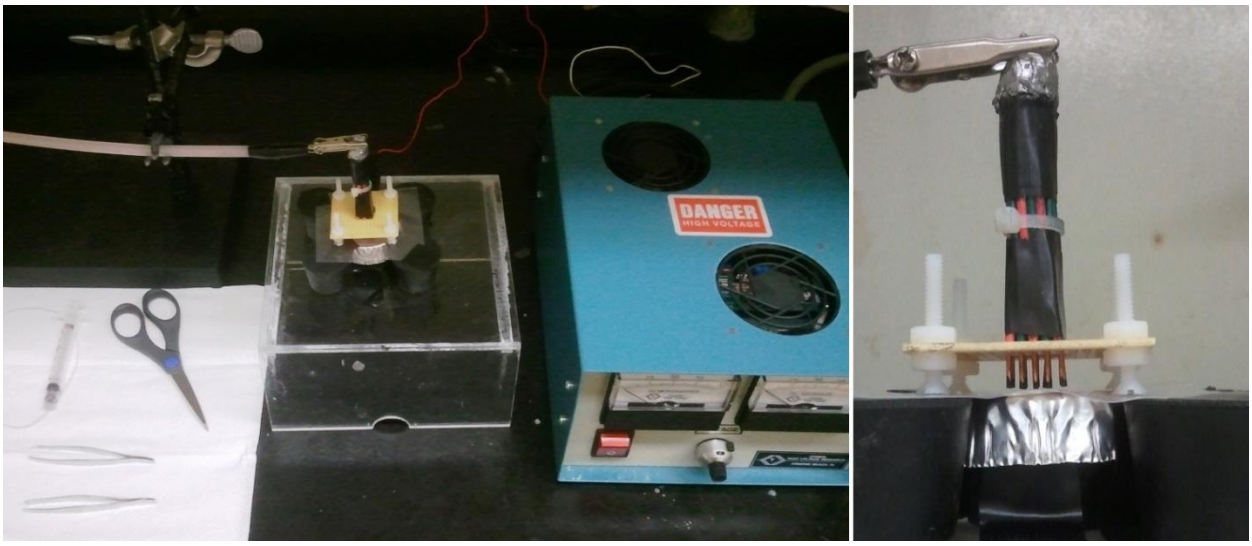

Figure 2-3: Electrowetting set up consisting of a power source, conductive platform and a dielectric layer separating the platform and the scaffold (left). Revised multi pin electrode used to electrowet (right).

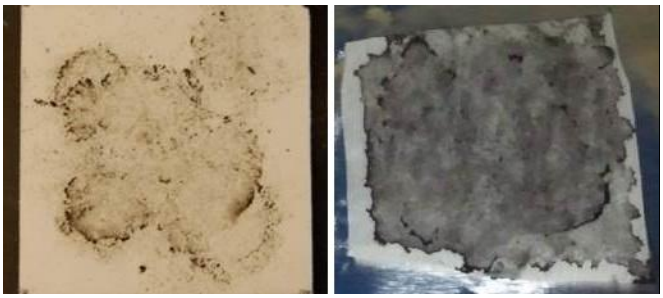

Figure 2-4: Effects of electrowetting with earlier prototype of multi pin electrode (left) and revised electrode (right).

II.5 Vacuum Impregnation

A vacuum impregnation method was explored to produce more uniformly wetted scaffolds. Although vacuum filtration methods have been tried in house in the past, they failed to successfully impregnate the pores. This may be on account of the underlying pore size of the filter which dictates the distributive negative pressure across the scaffold. While using a 0.2 micron pore filter (Nalgene Analytical Filter, 150 ml) successful trials of wetting were accomplished. A two by two inch polymer scaffold was placed on the filter and fixed in place with the upper cup of the filter. A volume of 3 mL of dispersion

was dispensed to cover the entire top surface of the exposed scaffold. When the vacuum is applied, the pressure difference forces the dispersion into the scaffolding. Successful trials of wetting were accomplished with filters of this pore size. Visual inspection indicates that the dispersion penetrated through the scaffold to the bottom.

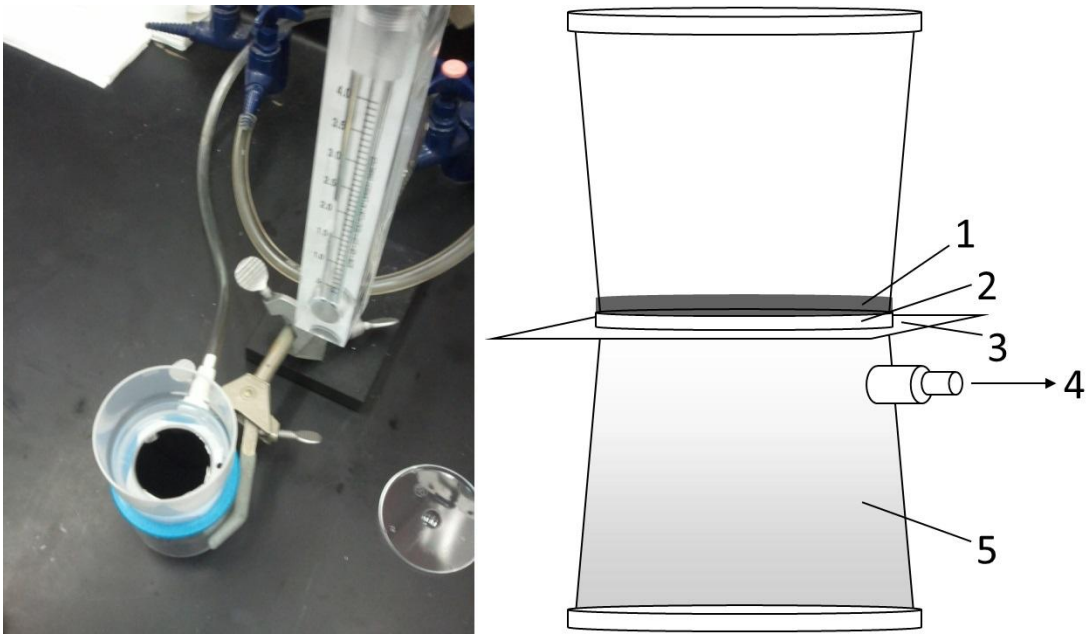

Figure 2-5: Vacuum impregnation set up includes a 0.2 micron filter connected to a flow gauge and vacuum line (left). Right schematic shows CNT dispersion (1), 0.2 µm filter (2), PLGA scaffold (3), vacuum nozzle (4), and Nalgene filter (5).

II.6 Scaffold Characterization

Vacuum impregnation was used to fabricate a variety of scaffolds. Dispersions with different concentrations of SWNT (0.4%, 0.2%, 0.1%, and 0.05%) were used to explore the different wetting effects and resulting scaffold properties (**Figure 2-6**). In another experiment, the filter was also tilted to produce a gradient of dispersion in the scaffold. Scaffold characterization methods for these samples include scanning electron microscopy (SEM), Raman spectroscopy and conductivity measurements.

Figure 2-6: Vacuum impregnated scaffolds with dispersions of varying CNT concentrations of 0.4%, 0.2%, 0.1% and 0.05% from left to right.

After allowing the wetted scaffolds to dry, SEM images were taken. A comparison of the scaffolds before and after impregnation confirmed successful wetting. A change in morphology can be seen going from smooth fibers to those with a rougher morphology (**Figure 2-7**). This is attributed to the presence of aggregates strongly adsorbed onto the fibers via van der Waals forces. A change in contrast in the scaffold can also be seen in the presence of SWNT. This demonstrates that SWNTs remain adsorbed to the scaffold surface after drying. SEM imaging of the bottom of the scaffold also validate complete penetration of the dispersion. Some filming also occurred on scaffolds with a SWNT concentration greater than 0.1%. It can be seen that a SWNT concentration of 0.05% maintained a very similar topography as the plain PLGA scaffold (**Figure 2-8**).

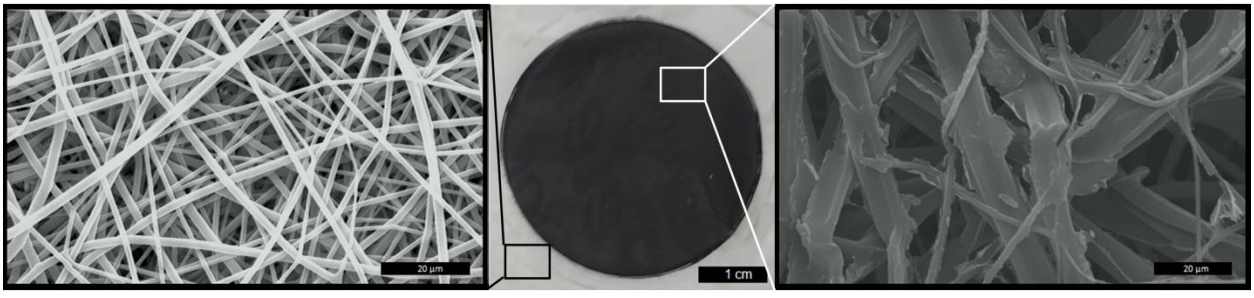

Figure 2-7: Wetted scaffold result from vacuum impregnation method (middle). SEM imaging of electrospun PLGA scaffold (left) and after implementation of CNT (right) with scale bar of 20 µm.

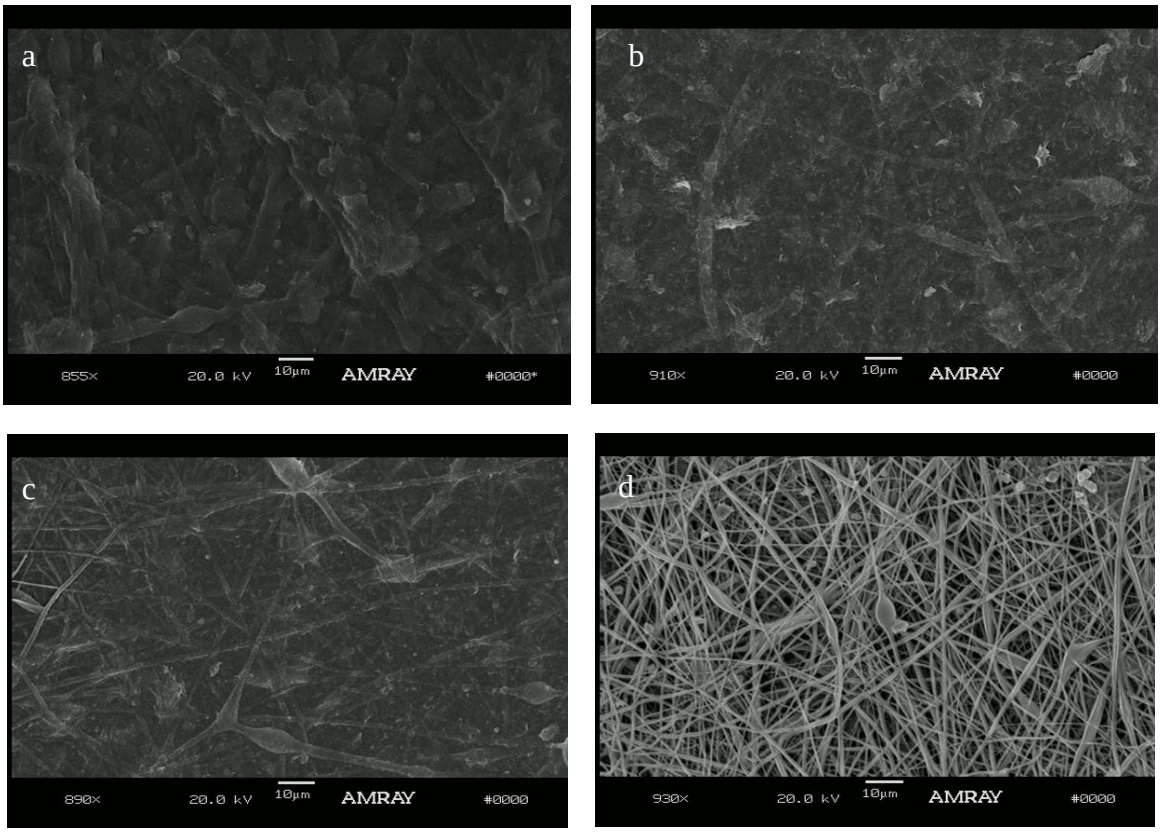

Figure 2-8: SEM images of scaffolds with dispersions of varying CNT concentrations of 0.4% (a), 0.2% (b), 0.1% (c) and 0.05% (d). Filming appears to occur on scaffolds with SWNT concentrations greater than 0.1%.

Contact angles were measured to explore the change in hydrophobicity on the surface of the scaffold before and after wetting. An image of a droplet of distilled water on each scaffold was analyzed in ImageJ software (**Figure 2-9**). The PLGA and SWNT-PLGA scaffolds had a contact angle of 117 and 80 degrees respectively. Resistance was also measured on scaffolds containing different concentrations of SWNT at four random coordinates on the each scaffold 1cm apart on each side (**Figure 2-10**). The 0.4% SWNT-PLGA scaffolds had consistent results on both sides pointing to a more complete wetting of the scaffold while maintaining a low overall resistance. The 0.05% scaffolds had a substantially higher level of resistance, but still could provide enough conductivity to be used in future cell differentiation work. Concentrations above 0.1% had similar

conductivity most likely do to the filming that occurs on the surface of the scaffolds for these concentrations.

Figure 2-9: Contact angles for PLGA (left) and SWNT-PLGA (right) scaffolds with a contact angle of 117 and 80 degrees respectively.

SWNT Concentration	Top (kΩ)	Bottom (kΩ)
0.40%	6.713	9.163
0.20%	1.784	53.79
0.10%	5.083	16.90
0.05%	677.5	564.2

Figure 2-10: Resistance measurements of top and bottom of SWNT-PLGA scaffolds.

Raman was not only used to confirm the presence, but also the integrity of the SWNTs. Raman spectroscopy emits a laser of wave length 633 nm (in this case) causing a shift in the photons as they hit the sample. This Raman shift gives information about the vibrational modes of the SWNTs. Different peak distributions from the Raman shift are unique for isolated, unfunctionalized SWNT [22, 23]. These Raman features include the radial breathing mode (RBM), tangential mode (G-band), the disorder induced D-band, and an overtone mode (G'-band). The RBMs correspond to the vibration of C atoms in the radial direction and appear between 150 cm^{-1} and 300 cm^{-1} depending on the nanotube diameter. A higher intensity can be attributed to unfunctionalized nanotubes. The G-band appears around 1600 cm^{-1} and provides information about whether the SWNTs are more semiconducting or metallic. Finally, a large D-band (~1300 cm^{-1}) with

respect to the G-band is an indication of amorphous carbon. Raman results showed excellent integrity of the SWNT in the scaffolds for each concentration (**Figure 2-11**). Peaks unique to SWNTs confirm that the BSA was able to deaggregate the tubes while maintaining a non-functionalized characteristic. Very little amorphous carbon was also confirmed, showing that sonication and the wetting procedure did not have any negative effects towards the integrity of the SWNTs. A lower G- peak relative to the G+ peak in the G-band for the SWNT-PLGA scaffold of 0.05% points to a more semiconducting than metallic nature of the nanotubes. This is an indication of less aggregation most likely do to a lack of filming which occurs on the scaffolds of higher concentrations.

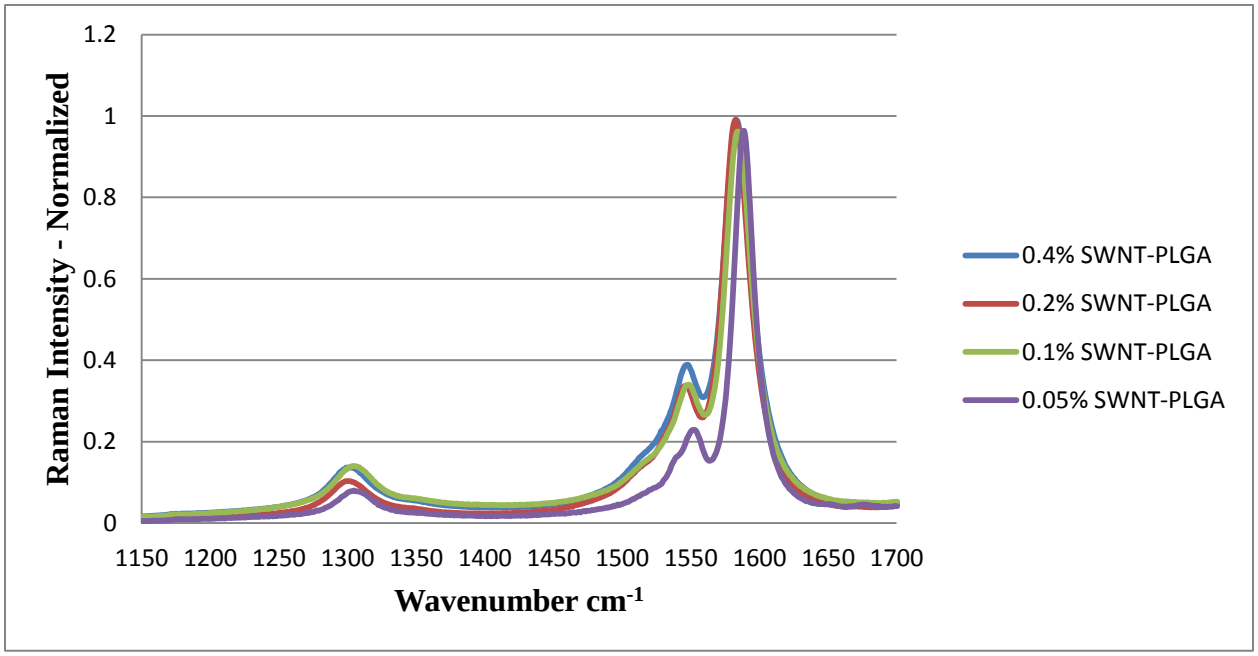

Figure 2-11: Normalized G-Band and D-Band Raman spectroscopy results for SWNT-PLGA scaffolds for each concentration at 633 nm.

II.7 Gradient Scaffolds

One of the primary goals in stem cell therapy is the enlistment of nearby matured cells and stem cells to damaged tissue with a guided approach [24]. How these cells

migrate depends on the in vivo microenvironment. The various physical, chemical and biological cues provide signals that guide the adhesion, migration, proliferation, differentiation and apoptosis of cells at certain locations and times [25]. The use of gradient materials may lead to the enhancement of desired cell mechanisms in addition to gaining insight in how these cells behave in vivo. It was first suggested by Ramon et al. that gradient materials could assist growing axons to their desired targets [26]. In the past few decades investigators began to implement a gradient into biomaterials. Doing so has proceeded through top down approaches (plasma [27], corona discharge [28], ultra-violet irradiation [29], chemical degradation [30]) as well as bottom-up approaches (infusion [31], diffusion [32], microcontact printing [33], microfluidic lithography [34], electrochemical method [35]).

Here, a top down approach was used to create a gradient by tilting the filter apparatus at an angle during impregnation. This causes a concentration gradient of the carbon nanotubes to run axial across the impregnated scaffold (**Figure 2-12**). This gradient will allow for the resistance to vary across the scaffold producing a voltage/current gradient during electrical stimulation. The extent of the gradient is characterized by thermal gravimetric analysis (TGA) and Raman spectroscopy (**Figure 2-13**). This allows one to identify which region of the scaffold enjoys the greatest cell viability, differentiation and neurite outgrowth, and therefore better optimization of the impregnated materials.

Figure 2-12: Gradient scaffolds impregnated at 5.5 º, 11º, and 15º.

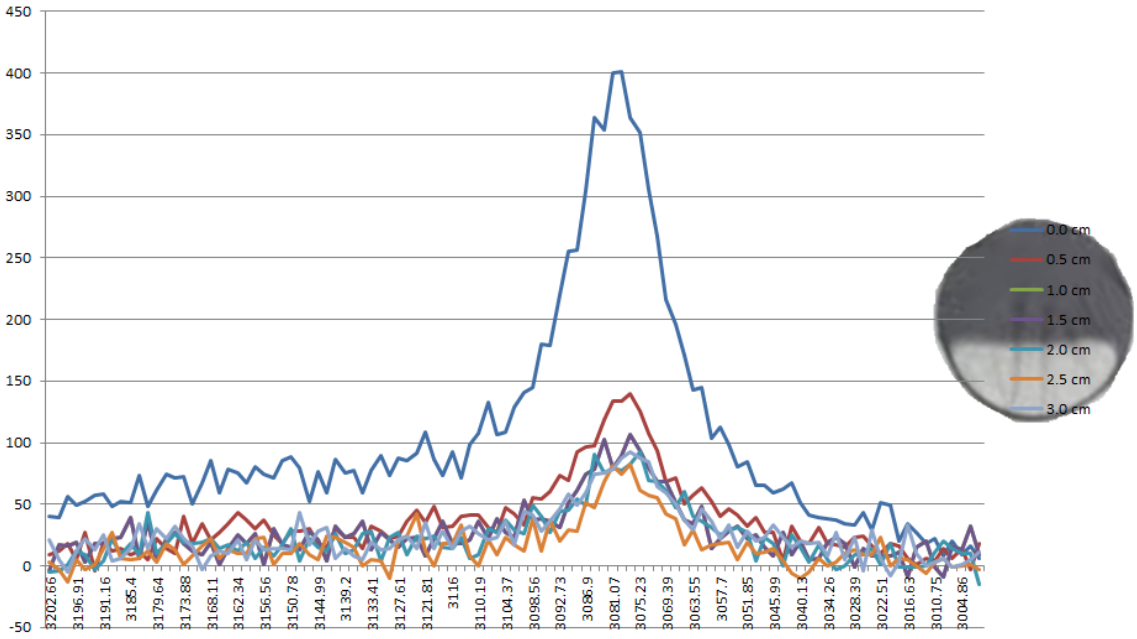

Figure 2-13: Raman spectroscopy of gradient scaffold.

Chapter III – Biological Application

III.1 Applications in Neural Tissue Engineering

The pluripotent capabilities of human embryonic stem cells (hESC) allow them to differentiate into a wide variety of cell types [36-38] including human neural stem cells (hNSCs). hNSCs are of particular interest for their ability to be differentiated into neurons for brain repair and neural regeneration. Despite this, hNSC applications are hindered by the lack of biomaterials that can promote cell adhesion, survival, and differentiation while also integrating neuronal stimulatory cues. Electrospun scaffolds can provide topographical cues to cells by supplying an in vitro mimic of the structure of the ECM and are capable of enhancing neurite outgrowth and neuronal differentiation of several cell types, including embryonic stem cells and hESC-derived NSCs [39-42]. Conductive substates can provide electrical shortcuts between developing cells and allow an applied electrical stimuli that can mimic the electrophysiological environment experienced by cells in a variety of biological processes, including muscle contraction, wound healing, and synaptic transmission [43-48]. This applied electrical stimulation can enhance neurite outgrowth, neuronal maturation, and may also direct neural stem cell migration, opening the possibility to guide these cells towards injured sites [48]. By making an electrospun scaffold conductive, all of the advantages could be combined into a single substrate.

The electrically conductive nature of nano carbon materials makes them a promising alternative for biological applications since metals can produce unwanted byproducts in the body. In particular, SWNT have been employed due to their inherently high conductivity and the ability to regulate neuronal behavior both structurally and

functionally [49]. Along with their biocompatibility at low concentrations, SWNT are ideal candidates for biomedical composites [5, 50]. SWNT interfaced with neural cells have also been shown to promote neuron growth [51-53] and can enhance differentiation of NSCs into neurons [6, 7, 54, 55]. Carbon nanotubes have also been used for biosensors [56], drug delivery [57] and the incorporation into composites [58]. The materials developed here focus on neural tissue engineering and stem cell differentiation.

III.2 Human Neural Stem Cell Cultures on Composite Scaffolds

The study done in this thesis is the first demonstration of electrically actuated CNT-based scaffolds for differentiation of human neural stem cells. Three scaffold conditions were tested: SWNT-PLGA scaffolds, PLGA scaffolds, and a 2D control of PLGA thin film glass coverslips. Scaffolds were sterilized with oxygen plasma and pretreated with laminin and poly-D-lysine to promote cell adhesion and neurite outgrowth. The hNSCs were primed for neuronal differentiation and seeded onto the scaffolds. One day after cell seeding, cells were labeled with calcein AM and propidium iodide to evaluate cell viability. The result showed significantly greater cell viability on the SWNT-PLGA and 2D control than on the PLGA scaffolds.

Immunocytochemistry and qRT-PCR was used to evaluate the neuronal differentiation. In 1, 7, and 14 day intervals during differentiation within the scaffolds, neuronal differentiation was characterized by evaluating Neurofilament M (NFM) and microtubule-associated protein 2 (MAP2) expressions. These two proteins are commonly found in soma and dendrites of neurons, respectively. They also play a critical role in the maintenance of the neuronal architecture, cellular differentiation, and structural and functional plasticity [59, 60]. The primary antibodies used to evaluate the presence of

NFM and MAP2 were anti-NFM (Invitrogen) and anti-MAP2 (Becton Dickinson), respectively. Cell nuclei were labeled with DAPI. Images were taken with the Leica SP2 confocal microscope and quantified using ImageJ software. The qRT-PCR analysis MAP2 was evaluated for undifferentiated NSCs after 14 days of differentiation for each scaffold condition.

After 7 days, 17% NFM positive cells and 17% MAP2 positive cells were observed in the SWNT-PLGA scaffolds, compared to 4% NFM positive cells and 9% MAP2 positive cells in the PLGA scaffolds. After 14 days, these numbers increased to 28% NFM positive cells and 23% MAP2 positive cells in the SWNT-PLGA scaffolds with 10% NFM positive cells and 10% MAP2 positive cells in PLGA scaffolds. This shows a clear difference in scaffolds with and without SWNT. The mature neuronal marker synaptophysin is a synaptic vesicle protein and was expressed in both scaffold conditions after 14 days. qRT-PCR also showed an increase in the expression of MAP2.

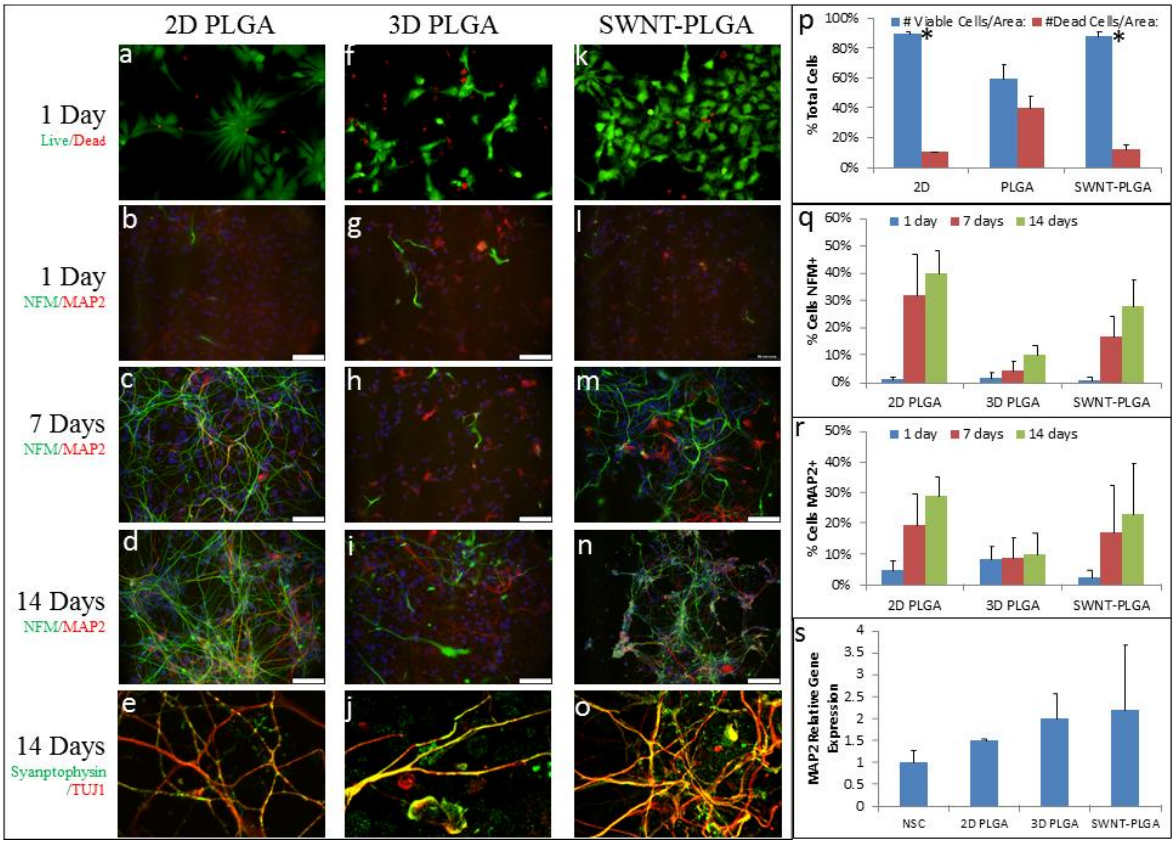

Figure 3-1: SWNT-PGLA scaffold differentiation results. SWNT-PLGA scaffolds elicit enhanced neuronal differentiation of hNSCs. hNSCs were cultured on 2D PLGA coverslips (a-e), PLGA scaffolds (f-j) and SWNT-PLGA scaffolds (k-o) to determine the effect of SWNT vacuum impregnation on hNSC differentiation and viability. The cells were labeled as live (green) or dead (red) after 1 day of scaffold growth (a, f, & k). These cells were labeled using for antibodies NFM (green) and MAP2 (red) at 1, 7, and 14 days in the scaffold (b-d, g-h, & l-o) and for Synaptophysin (green) and TUJ1 (red) at 14 days in the scaffold (e, j & o). Mature, punctate Synaptophysin can be seen in the neurites and cell bodies of the cells of both conditions at day 14. The percentage of cells positive for NFM and MAP2 markers are shown (i & j). PCR was performed to assay the fold gene expression of MAP2 (k).

III.3 Electrical Stimulation of hNCS on SWNT-PLGA Scaffolds

While conductive substrates alone have been previously shown to enhance neuronal differentiation, applied electrical stimulation can also modulate cell and tissue growth in nerve cultures [61] and for the differentiation of myoblasts [62]. However, the combination of the electrospun scaffolds with applied electrical stimulation has yet to be explored for hNSCs. We hypothesized that the SWNT-PLGA scaffolds could deliver an

electrical stimulus to cultured hNSCs, and that this electrical stimulation would further enhance neuronal differentiation.

A custom circuit board was designed to support the electrical stimulation of up to eight samples simultaneously (**Figure 3-2**). The middle portion of an indium tin oxide (ITO) covered glass slide is etched with a solution of 20% HCl and 5% HNO_3 to create a non-conductive gap between two electrodes [63]. A scaffold sample is large enough to bridge the gap ensuring that the applied current travels through the SWNT scaffold. The SWNT scaffolds are fitted with cell culture rings that house the cells and growth media. The power source consists of a 2.5 volt watch battery. The ITO glass slides had a resistance of 200 Ω (+/- 50 Ω) whereas the scaffold contained a resistance of 5 kΩ (+/- 2.5 kΩ) on the top and 15 kΩ (+/- 5 kΩ) on the bottom, respectively. An electrical stimulation of 30 µA direct current was applied to the cells for 10 minutes on the third day of differentiation under the experimental conditions.

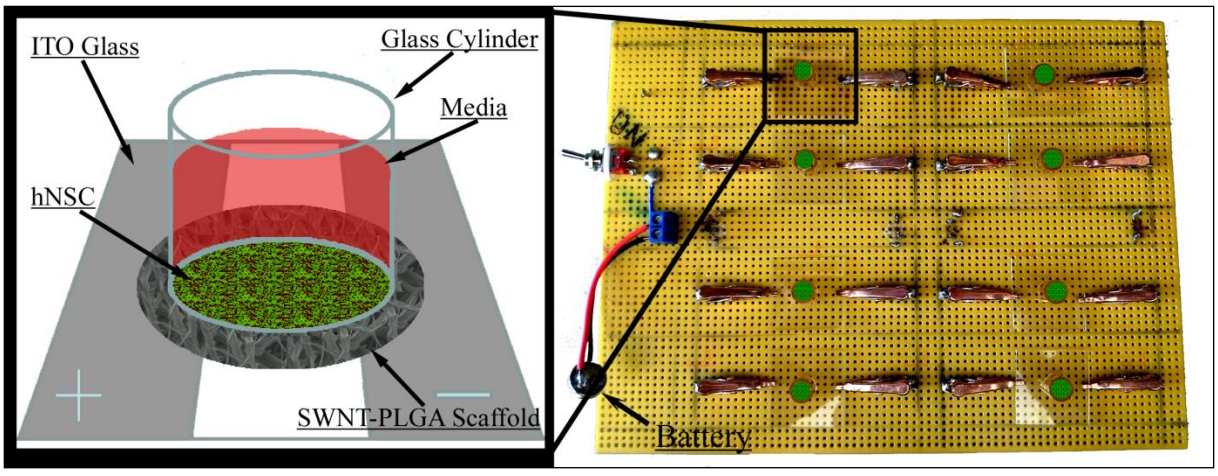

Figure 3-2: Electrical stimulation schematic showing a single scaffold on an etched ITO glass slide. Current flows from the positive electrode through the scaffold to the negative electrode. A culture ring is attached to contain the cell media. To the right is a diagram of a series circuit with the ability to stimulate up to 8 scaffolds simultaneously.

Tests on day 1 cultures showed that the electrical stimulation had a negligible effect on cell viability and the total cell number. After 14 days, NSC differentiation was evaluated for samples with and without electrical stimulation. Although percentage of MAP2 positive cells did not increase, electrical stimulation was increased MAP2 gene expression. Previous reports have demonstrated in vivo that electrical stimulation can increase MAP2 expression, which can in turn increase dendritic and synaptic plasticity [64]. Electrical stimulation also increased the number of NFM positive cells increased from 28% to 32% of cells. It is interesting to note that the change in MAP2 and NFM expression relative to un-stimulated samples shows a somewhat delayed but sustained effect on the expression of these cytoskeletal proteins. Though the exact mechanisms are not understood, it is likely that the stimulation activates a pathway far upstream of MAP2 or dendrite formation. It could also induce differences in secondary remodeling phenomena, which results in longer term effects on neuronal differentiation. Notably, we have also observed that the network connectivity in SWNT-PLGA scaffolds resulted in an increased calcium influx response to an electrical stimulation.

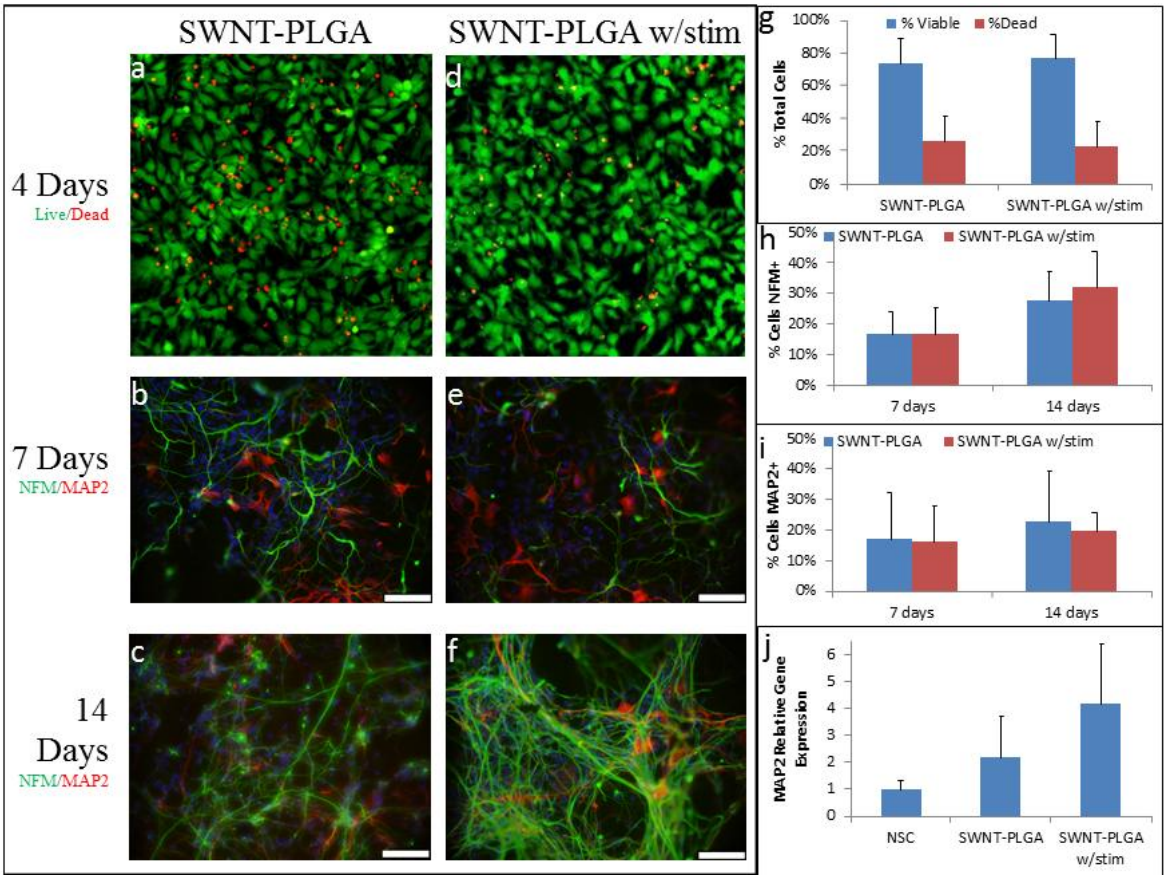

Figure 3-3: Differentiation results with electrical stimulation. Stimulation further enhances neuronal differentiation of hNSCs in SWNT-PLGA scaffolds. hNSCs were cultured on SWNT-PLGA scaffolds, and at day 3, selected scaffolds were electrically stimulated for ten minutes at 30μA. The day after that stimulation, a subset were labeled as live (green) or dead (red) (a & d). The number of live and dead cells was quantified (g). After 7 and 14 days, the cells were fixed and all conditions were labeled with antibodies for NFM (green) and MAP2 (red) (b-c & e-f). The percentage of NFM and MAP2 cells for each condition are shown (h & i), at 14 days the percentage of MAP2 cells trends upwards following electrical stimulation. PCR analysis of MAP2 gene fold expression (j) has an upward trend following electrical stimulation.

Chapter IV – Conclusions and Future Perspectives

Electrospun SWNT-PLGA scaffolds with high surface area and electrical conductivity were produced by vacuum-driven impregnation of an electrospun fibrous scaffold with SWNT dispersion. The scaffolds combined the advantageous features of highly conductive SWNTs with the topology of electrospun scaffolds and were found to be highly biocompatible for support of hNSCs. These scaffolds can increase the kinetics of hNSC neuronal differentiation and maturation, which is further accelerated through the application of electrical stimulation.

These substrates could be vital for in vitro applications using patient-derived induced pluripotent stem cells. Such a system could be used to transplant human neuronal cells to spinal cord or brain injury sites and serve to accelerate neuronal differentiation, improve integration of exogenous cells within the host tissue, and provide the ability to deliver or monitor electrical signals to or from the transplanted constructs. In addition, interfacing human neuronal cells with these SWNT-PLGA scaffolds opens up a wide range of applications to testing the plasticity, functionality, and subtype specificity of neurons following programmed regimen of electrical stimulation. Thus, the composite scaffolds present promising candidates for probing neurogenesis and neural activity, given the high levels of biocompatibility, three-dimensional geometries, extracellular matrix-mimetic topography, and tunable differentiation/maturation cues.

References

1. Kroto, H.W., et al., *C-60 - Buckminsterfullerene.* Nature, 1985. **318**(6042): p. 162-163.
2. Iijima, S., *Helical Microtubules of Graphitic Carbon.* Nature, 1991. **354**(6348): p. 56-58.
3. Novoselov, K.S., et al., *Electric field effect in atomically thin carbon films.* Science, 2004. **306**(5696): p. 666-669.
4. Collins, P.G. and P. Avouris, *Nanotubes for electronics.* Scientific American, 2000. **283**(6): p. 62-+.
5. Dubin, R.A., et al., *Carbon nanotube fibers are compatible with mammalian cells and neurons.* Ieee Transactions on Nanobioscience, 2008. **7**(1): p. 11-14.
6. Jan, E. and N.A. Kotov, *Successful differentiation of mouse neural stem cells on layer-by-layer assembled single-walled carbon nanotube composite.* Nano Letters, 2007. **7**(5): p. 1123-1128.
7. Ni, Y.C., et al., *Chemically functionalized water soluble single-walled carbon nanotubes modulate neurite outgrowth.* Journal of Nanoscience and Nanotechnology, 2005. **5**(10): p. 1707-1712.
8. Thostenson, E.T., Z.F. Ren, and T.W. Chou, *Advances in the science and technology of carbon nanotubes and their composites: a review.* Composites Science and Technology, 2001. **61**(13): p. 1899-1912.
9. Iijima, S. and T. Ichihashi, *SINGLE-SHELL CARBON NANOTUBES OF 1-NM DIAMETER.* Nature, 1993. **363**(6430): p. 603-605.
10. O'Connell, M.J., et al., *Reversible water-solubilization of single-walled carbon nanotubes by polymer wrapping.* Chemical Physics Letters, 2001. **342**(3-4): p. 265-271.
11. Matsuura, K., et al., *Selectivity of water-soluble proteins in single-walled carbon nanotube dispersions.* Chemical Physics Letters, 2006. **429**(4-6): p. 497-502.
12. Valenti, L.E., et al., *The adsorption-desorption process of bovine serum albumin on carbon nanotubes.* Journal of Colloid and Interface Science, 2007. **307**(2): p. 349-356.
13. Elgrabli, D., et al., *Effect of BSA on carbon nanotube dispersion for in vivo and in vitro studies.* Nanotoxicology, 2007. **1**(4): p. 266-278.
14. Lim, S.H. and H.Q. Mao, *Electrospun scaffolds for stem cell engineering.* Advanced Drug Delivery Reviews, 2009. **61**(12): p. 1084-1096.
15. Agic, A. and B. Mijovic, *Mechanical properties of electrospun carbon nanotube composites.* Journal of the Textile Institute, 2006. **97**(5): p. 419-427.
16. Kannan, P., S.J. Eichhorn, and R.J. Young, *Deformation of isolated single-wall carbon nanotubes in electrospun polymer nanofibres.* Nanotechnology, 2007. **18**(23): p. 7.
17. Liu, Y., et al., *Bio-nanowebs based on poly(styrene-beta-isobutylene-beta-styrene) (SIBS) containing single-wall carbon nanotubes.* Chemistry of Materials, 2007. **19**(11): p. 2721-2723.
18. Salalha, W., et al., *Single-walled carbon nanotubes embedded in oriented polymeric nanofibers by electrospinning.* Langmuir, 2004. **20**(22): p. 9852-9855.
19. Sundaray, B., et al., *Preparation and Characterization of Electrospun Fibers of Poly(methyl methacrylate) - Single Walled Carbon Nanotube Nanocomposites.* Journal of Engineered Fibers and Fabrics, 2008. **3**(4): p. 39-45.
20. Quilliet, C. and B. Berge, *Electrowetting: a recent outbreak.* Current Opinion in Colloid & Interface Science, 2001. **6**(1): p. 34-39.
21. Yeo, L. and H.-C. Chang, *Electrowetting*, in *Encyclopedia of microfluidics and nanofluidics*, D. Li, Editor. 2008, Springer: New York. p. 600-606.

22. Dresselhaus, M.S., et al., *Raman spectroscopy of carbon nanotubes.* Physics Reports-Review Section of Physics Letters, 2005. **409**(2): p. 47-99.
23. Sethi, R. and A.R. Barron, *Characterization of Single-Walled Carbon Nanotubes by Raman Spectroscopy.* Connexions Web site, 2009.
24. Godwin, J.W. and J.P. Brockes, *Regeneration, tissue injury and the immune response.* Journal of Anatomy, 2006. **209**(4): p. 423-432.
25. Jagur-Grodzinski, J., *Polymers for tissue engineering, medical devices, and regenerative medicine. Concise general review of recent studies.* Polymers for Advanced Technologies, 2006. **17**(6): p. 395-418.
26. Wu, J.D., et al., *Gradient biomaterials and their influences on cell migration.* Interface Focus, 2012. **2**(3): p. 337-355.
27. Spijker, H.T., et al., *Protein adsorption on gradient surfaces on polyethylene prepared in a shielded gas plasma.* Colloids and Surfaces B-Biointerfaces, 1999. **15**(1): p. 89-97.
28. Shin, Y.N., et al., *Adhesion comparison of human bone marrow stem cells on a gradient wettable surface prepared by corona treatment.* Applied Surface Science, 2008. **255**(2): p. 293-296.
29. Li, B., et al., *A technique for preparing protein gradients on polymeric surfaces: effects on PC12 pheochromocytoma cells.* Biomaterials, 2005. **26**(13): p. 1487-1495.
30. Zhu, Y.B., et al., *Endothelium regeneration on luminal surface of polyurethane vascular scaffold modified with diamine and covalently grafted with gelatin.* Biomaterials, 2004. **25**(3): p. 423-430.
31. Tomlinson, M.R. and J. Genzer, *Formation of grafted macromolecular assemblies with a gradual variation of molecular weight on solid substrates.* Macromolecules, 2003. **36**(10): p. 3449-3451.
32. Chaudhury, M.K. and G.M. Whitesides, *HOW TO MAKE WATER RUN UPHILL.* Science, 1992. **256**(5063): p. 1539-1541.
33. Childs, W.R. and R.G. Nuzzo, *Decal transfer microlithography: A new soft-lithographic patterning method.* Journal of the American Chemical Society, 2002. **124**(45): p. 13583-13596.
34. Irimia, D., D.A. Geba, and M. Toner, *Universal microfluidic gradient generator.* Analytical Chemistry, 2006. **78**(10): p. 3472-3477.
35. Righetti, P.G. and A. Bossi, *Isoelectric focusing in immobilized pH gradients: an update.* Journal of Chromatography B, 1997. **699**(1-2): p. 77-89.
36. Keller, G., *Embryonic stem cell differentiation: emergence of a new era in biology and medicine.* Genes & Development, 2005. **19**(10): p. 1129-1155.
37. Murry, C.E. and G. Keller, *Differentiation of embryonic stem cells to clinically relevant populations: Lessons from embryonic development.* Cell, 2008. **132**(4): p. 661-680.
38. Thomson, J.A., et al., *Embryonic stem cell lines derived from human blastocysts.* Science, 1998. **282**(5391): p. 1145-1147.
39. Cherry, J.F., et al., *Oriented, Multimeric Biointerfaces of the L1 Cell Adhesion Molecule: An Approach to Enhance Neuronal and Neural Stem Cell Functions on 2-D and 3-D Polymer Substrates.* Biointerphases, 2012. **7**(1-4).
40. Christopherson, G.T., H. Song, and H.Q. Mao, *The influence of fiber diameter of electrospun substrates on neural stem cell differentiation and proliferation.* Biomaterials, 2009. **30**(4): p. 556-564.
41. Lu, H.F., et al., *Efficient neuronal differentiation and maturation of human pluripotent stem cells encapsulated in 3D microfibrous scaffolds.* Biomaterials, 2012. **33**(36): p. 9179-9187.

42. Xie, J.W., et al., *The differentiation of embryonic stem cells seeded on electrospun nanofibers into neural lineages.* Biomaterials, 2009. **30**(3): p. 354-362.
43. Cellot, G., et al., *Carbon Nanotube Scaffolds Tune Synaptic Strength in Cultured Neural Circuits: Novel Frontiers in Nanomaterial-Tissue Interactions.* Journal of Neuroscience, 2011. **31**(36): p. 12945-12953.
44. Cho, Y.N. and R. Ben Borgens, *The effect of an electrically conductive carbon nanotube/collagen composite on neurite outgrowth of PC12 cells.* Journal of Biomedical Materials Research Part A, 2010. **95A**(2): p. 510-517.
45. Geremia, N.M., et al., *Electrical stimulation promotes sensory neuron regeneration and growth-associated gene expression.* Experimental Neurology, 2007. **205**(2): p. 347-359.
46. Graves, M.S., et al., *Electrically Mediated Neuronal Guidance with Applied Alternating Current Electric Fields.* Annals of Biomedical Engineering, 2011. **39**(6): p. 1759-1767.
47. Luo, X.L., et al., *Highly stable carbon nanotube doped poly(3,4-ethylenedioxythiophene) for chronic neural stimulation.* Biomaterials, 2011. **32**(24): p. 5551-5557.
48. McCaig, C.D., et al., *Controlling cell behavior electrically: Current views and future potential.* Physiological Reviews, 2005. **85**(3): p. 943-978.
49. Fabbro, A., et al., *Carbon Nanotubes: Artificial Nanomaterials to Engineer Single Neurons and Neuronal Networks.* Acs Chemical Neuroscience, 2012. **3**(8): p. 611-618.
50. Lewitus, D.Y., et al., *Biohybrid Carbon Nanotube/Agarose Fibers for Neural Tissue Engineering.* Advanced Functional Materials, 2011. **21**(14): p. 2624-2632.
51. Alexander, J.K., B. Fuss, and R.J. Colello, *Electric field-induced astrocyte alignment directs neurite outgrowth.* Neuron Glia Biology, 2006. **2**: p. 93-103.
52. Gordon, T., et al., *Brief Electrical Stimulation Accelerates Axon Regeneration in the Peripheral Nervous System and Promotes Sensory Axon Regeneration in the Central Nervous System.* Motor Control, 2009. **13**(4): p. 412-441.
53. Wood, M.D. and R.K. Willits, *Applied electric field enhances DRG neurite growth: influence of stimulation media, surface coating and growth supplements.* Journal of Neural Engineering, 2009. **6**(4): p. 8.
54. Chao, T.I., et al., *Carbon nanotubes promote neuron differentiation from human embryonic stem cells.* Biochemical and Biophysical Research Communications, 2009. **384**(4): p. 426-430.
55. Sridharan, I., T. Kim, and R. Wang, *Adapting collagen/CNT matrix in directing hESC differentiation.* Biochemical and Biophysical Research Communications, 2009. **381**(4): p. 508-512.
56. Lin, Y.H., et al., *Glucose biosensors based on carbon nanotube nanoelectrode ensembles.* Nano Letters, 2004. **4**(2): p. 191-195.
57. Bianco, A., K. Kostarelos, and M. Prato, *Applications of carbon nanotubes in drug delivery.* Current Opinion in Chemical Biology, 2005. **9**(6): p. 674-679.
58. Sinha, N. and J.T.W. Yeow, *Carbon nanotubes for biomedical applications.* Ieee Transactions on Nanobioscience, 2005. **4**(2): p. 180-195.
59. Xiong, Y., et al., *Synaptic transmission of neural stem cells seeded in 3-dimensional PLGA scaffolds.* Biomaterials, 2009. **30**(22): p. 3711-22.
60. Zhang, N., et al., *Effects of salvianolic acid B on survival, self-renewal and neuronal differentiation of bone marrow derived neural stem cells.* Eur J Pharmacol, 2012. **697**(1-3): p. 32-9.
61. Park, S.Y., et al., *Enhanced Differentiation of Human Neural Stem Cells into Neurons on Graphene.* Advanced Materials, 2011. **23**(36): p. H263-+.

62. Quigley, A.F., et al., *Electrical stimulation of myoblast proliferation and differentiation on aligned nanostructured conductive polymer platforms.* Adv Healthc Mater, 2012. **1**(6): p. 801-8.
63. Gheith, M.K., et al., *Stimulation of neural cells by lateral layer-by-layer films of single-walled currents in conductive carbon nanotubes.* Advanced Materials, 2006. **18**(22): p. 2975-+.
64. Zhou, Q., et al., *Cortical electrical stimulation alone enhances functional recovery and dendritic structures after focal cerebral ischemia in rats.* Brain Res, 2010. **1311**: p. 148-57.